Journal of Particle Science and Technology 9 (2) (2023) 63-71

Iranian Research Organization for Science and Technology (IROST)

Journal of PARTICLE Science & Technology

JPST
https://jpst.irost.ir

Online ISSN: 2423-4079
Print ISSN: 2423-4087

Fabrication method, microstructural characteristics, and hardness behavior of an interpenetrating phases hybrid aluminum/alumina-nanodiamond composite

Hassan Zeinali Moghaddam, Ghodratollah Roudini✉, Hamed Khosravi

Department of Materials Engineering, Faculty of Engineering, University of Sistan and Baluchestan, Zahedan, Iran

HIGHLIGHTS

- Microstructure and hardness of interpenetrating phases hybrid aluminum/alumina-nanodiamond composites were investigated.
- A good distribution of diamond nanoparticles in the preform was observed.
- Increasing the volume percentage of diamond nanoparticles increased the hardness of the composite to 263.8 Vickers at 10 vol%.

GRAPHICAL ABSTRACT

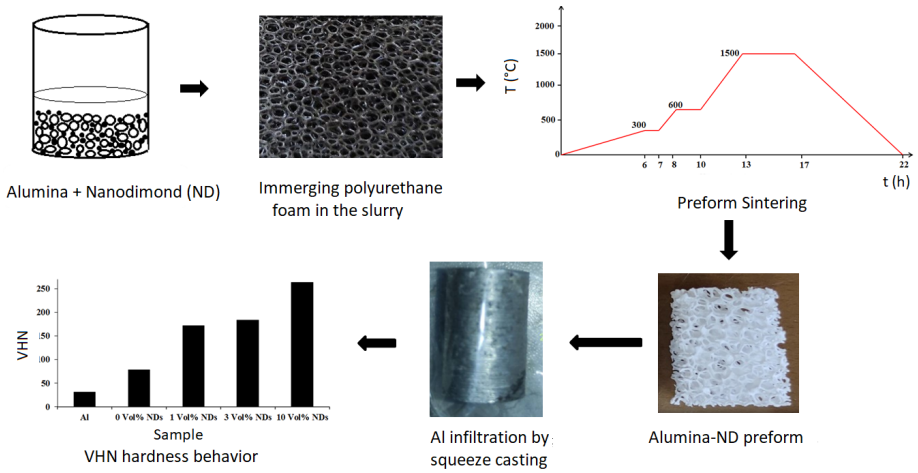

ARTICLE INFO

Article type:

Research article

Article history:

Received 17 October 2023
Received in revised form 18 September 2023
Accepted 19 September 2023

Keywords:

Aluminum-matrix composite
Interpenetrating phases
Nanodiamond
Microstructure
Hardness

DOI: 10.22104/JPST.2023.6538.1244

ABSTRACT

In the present work, the addition effects of nanodiamond (ND) on the microstructure and hardness behavior of interpenetrating phases hybrid Al/Al_2O_3 metal matrix composites were investigated. The fabrication of the composites was done via a two-step process. In the first step, hybrid Al_2O_3-ND preforms were prepared, and then molten pure Al alloy was infiltrated into the preforms. The preforms were fabricated by the replica method using a polyurethane foam and an Al_2O_3-ND slurry with various ND contents (0, 1, 3, and 10 vol%). The preforms were sintered at 1500 °C for 4 h under argon gas protection. Finally, the composites were fabricated by Al melt infiltration into the preforms via the squeeze casting method. The microstructure of the fabricated composites was analyzed using optical and scanning electron microscopes. The hardness of the composites was measured using a Vickers hardness tester. The results of the microstructural evaluations demonstrated a good distribution of ND in the preform. By increasing the ND content from 0 to 10 vol%, the matrix average grain size decreased from 143 µm to 76 µm. The results of the Vickers hardness test showed that increasing the volume percentage of ND increased the composite hardness to 263.8 Vickers at 10 vol%. The two main strengthening mechanisms for these composites are the Orowwn mechanism (volume fraction of ND particles) and the Hal-Petch mechanism (grain size), which affect the hardness behavior.

✉ *Corresponding author: E-mail address:* ghodratollah.roudini@eng.usb.ac.ir ; *Tel:* +9854-31136221 ; *Fax:* +9854-33447092

1. Introduction

Composite materials are fabricated using several traditional methods (e.g., casting, powder metallurgy, infiltration, etc.) by combining a matrix phase with one or more reinforcements [1]. In recent years, a new type of composite material has been fabricated in which both the matrix and reinforcement phases form a three-dimensional network. These composites are known as interpenetrating composites (IPCs) [2]. IPCs consist of topologically connected phases. Due to the continuity in both the matrix and reinforcements, this type of composite exhibits unique properties [3]. Several studies have been conducted on IPCs, primarily focusing on constructing composites with a metal matrix and continuous ceramic reinforcement [4,5]. These IPCs have demonstrated better mechanical strength and stiffness than particle-reinforced composites at both room and elevated temperatures. Additionally, the particular connection between the reinforcing particles essentially reduces the three-dimensional linkage between the reinforcement and the matrix, resulting in the development of multifunctional macroscopic properties [6].

The most important challenges in the fabrication of the IPCs are the connection and spatial distribution of the reinforcement components within two or more phases. The most commonly employed method for producing IPCs involves the infiltration of a molten metal phase into porous, open-cell ceramic preforms under pressure. The pressure is necessary due to the weak wettability of the ceramic preforms with molten metals. For this purpose, a certain level of mechanical stability in the ceramic foam and a well-connected open porous network with sufficient permeability are needed [7]. In general, the properties of the resulting composites depend on the mechanical and structural properties of ceramic preform [8]. To achieve a composite with desirable mechanical properties, a mechanically stable ceramic framework with an open porosity of more than 50%, coupled with a homogeneous pore size distribution, is essential [9]. Various methods have been employed to fabricate these ceramic preforms, including pressing and sintering ceramic powders [10], pore-forming processes [11], replica methods [12], gel casting [13], freeze casting [9], and 3D ink printing [14].

Open-cell ceramic foams serve as essential components in applications necessitating fluid transport through their structure. Some distinct characteristics of these foams are low bulk density, minimal thermal conductivity, low dielectric constant, and exceptional resistance to thermal shocks. However, in many applications, their brittleness makes them susceptible to failure when exposed to compressive loads. Remarkably, there is a notable scarcity of experimental data regarding the compression behavior of these fragile ceramic foams. Consequently, it has become imperative to obtain more information about the mechanisms of failure under compressive loads, paving the path for potential enhancements in both macro and microstructural designs [15].

Several research works have been done to investigate the various properties of interpenetrating phases metal matrix composites. For example, Roy *et al.* [16,17] investigated the elastic and thermal expansion behavior of interpenetrating Al12Si/alumina composites. The effect of reinforcement contiguity on the thermal expansion of Al_2O_3-Al composites was explored by Roudini *et al.* [18]. Kouzeli *et al.* [19] compared the compressive behavior of Al-matrix composites containing 34 and 37 vol% sub-micron Al_2O_3 for two various reinforcement architectures of interconnected and discontinuous.

One of the interesting reinforcements for metal matrix composites is nanodiamond due to its outstanding properties such as high strength, high charge mobility, high thermal conductivity (TC, ~1300-2000 $W.m^{-1}.K^{-1}$), and very low coefficient of thermal expansion (CTE, 1.2-3.5×10^{-6} K^{-1}) [20-22]. Some researchers have fabricated diamond-reinforced metal matrix composites and investigated their properties [23-26].

According to the literature, no research has been found regarding the hybrid nanodiamond/alumina-reinforced interpenetrating phases composite. Due to its good mechanical and thermal properties (thermal conductivity and thermal expansion), this kind of composite can be used as a structural and thermal management material. Thus, this work aimed to investigate the influence of diamond nanoparticles on the microstructural features and hardness behavior of the Al-Al_2O_3 hybrid interpenetrating phases composites. The non-homogeneous distribution and agglomeration of hybrid particles are disadvantages of these composites and may decrease their mechanical properties.

2. Experimental

2.1. The preform preparation process

Al_2O_3 particles with an average size of 1 μm and nanodiamond (ND) particles (Tech Diamond Tools Inc.) with an average size of 100 nm were utilized in Al_2O_3-ND slurry with various ND contents (0, 1, 3, and 10 vol%). The Al_2O_3 and ND particles were manually mixed for 10 min to achieve a better particle distribution. Subsequently, liquid egg white was added as a protein binder to the mixture of particles at a concentration of 4 vol%. The resulting slurry was manually stirred for 10 min to obtain a homogeneous distribution. In the subsequent step, polyurethane foam with an average pore size of 17 ppm was immersed in the slurry after being washed with acetone. The excess slurry was removed using a roller,

and this process was repeated three times to ensure complete foam coverage of the slurry.

The sintering process involved placing the foam in a tunnel furnace under argon gas. The heat treatment required for sintering the ceramic foam is depicted in Fig. 1. As it can be seen, the temperature was increased at a rate of 1 °C.min^{-1} to 300 °C and maintained for 1 h to facilitate the slow combustion of the polyurethane foam and its removal from the system. Subsequently, the temperature was increased at a rate of 2.5 °C.min^{-1} to 600 °C and held at this temperature for 2 h. For final sintering and densification, the temperature was raised to 1500 °C at a rate of 4 °C.min^{-1} and held at this temperature for 4 h, followed by cooling to ambient temperature at a rate of 10 °C.min^{-1}. The micro and macro images of the resulting preform are presented in Fig. 2. The average pore size was determined to be 2.432 mm using Image-J software.

2.2. The composite preparation process

A hot press squeeze casting process was employed to produce an Al/Al_2O_3-ND continuous matrix composite. The piston and cylinder were fabricated from plain carbon steel, and ceramic preform was placed inside the cylinder. Then, the piston and cylinder were placed in an electric furnace with pure Al, and the temperature was gradually increased to 750 °C at a rate of 10 °C.min^{-1}. The furnace was maintained at this temperature for 1 h to ensure isothermal melting. The squeeze casting process was then initiated by pouring the molten Al into the cylinder, placing the piston on top of the cylinder, and applying pressure using a press machine. The cylinder and piston assembly were cooled in water to direct solidification, and the sample was subsequently removed.

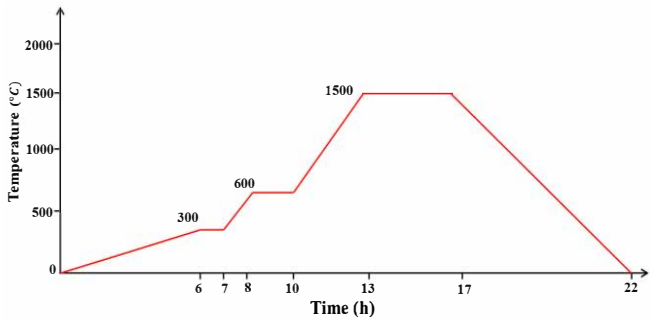

Fig. 1. The temperature-time cycle for the preform sintering process.

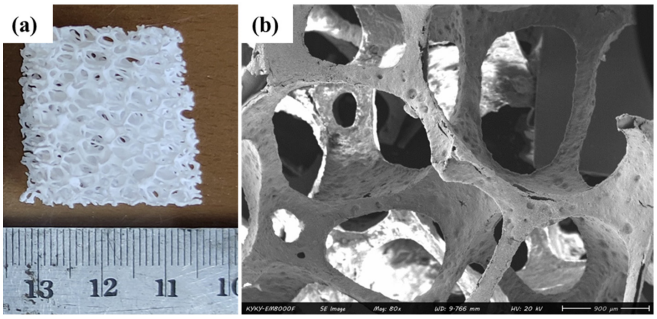

Fig. 2. (a) Macrograph and (b) SEM micrograph of the fabricated preform.

2.3. Characterization

To analyze the microstructure of the produced composites, the samples were cut and polished, followed by etching with a 0.5 % hydrofluoric acid solution [27]. A scanning electron microscope equipped with energy spectroscopy (FE-SEM/ KYKY-EM8000F) and an Olympus optical microscopy were utilized to characterize the microstructures. Finally, the microhardness of the samples was determined using an INNOVA TEST (Netherlands) Universal model microhardness tester.

3. Results and discussion

3.1. Microstructure

Fig. 3 shows FE-SEM images of the preforms fabricated with 3 and 10 vol% ND particles. According to Fig. 3(a), the

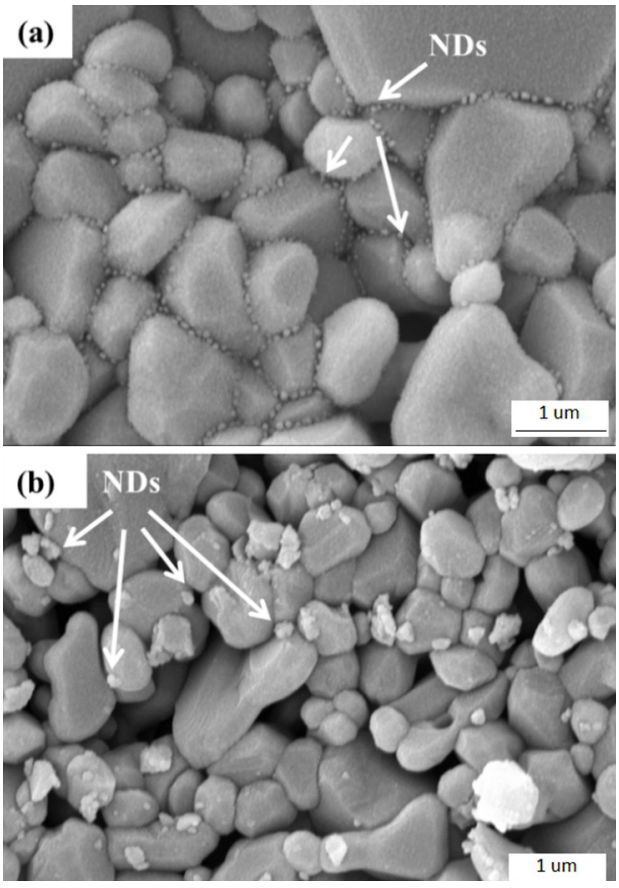

Fig. 3. ND distribution in the fabricated preform with (a) 3 and (b) 10 vol% ND.

sample containing 3 vol% ND exhibits a uniform and regular distribution of the ND among the Al_2O_3 particles. Upon closer inspection of the ceramic preform containing 10 vol% ND particles (Fig. 3(b)), it is clear that the ND particles adhere to each other, leading to agglomeration and an increase in voids between the Al_2O_3 particles.

To confirm the presence of ND particles in these foams, an elemental distribution map was obtained from the ceramic preform containing 10 vol% ND (Fig. 4). Regarding this figure, the ND distribution in the microstructure of the ceramic preform is evident.

Fig. 5 shows low-magnification FE-SEM micrographs from the interpenetrating phases hybrid Al/Al_2O_3-ND composites fabricated with various volume percentages of ND particles (0, 1, 3, and 10 vol%). The distribution of ND is related to the volume fraction of the hybrid reinforcements in the preforms. Higher magnification images were also prepared to show the distribution of the nanoparticles in the reinforcing phase, and the results are presented in Fig. 6. The dimension of the ND particles allows the observation of their distribution in the reinforcing phase. Furthermore, an elemental distribution map was also taken to better ensure the distribution of ND in the Al_2O_3 structure. Fig. 7 displays the elemental distribution map of the composite containing 10 vol% ND. The carbon distribution demonstrates the appropriate distribution of ND in the reinforcement structure.

Fig. 8 shows the optical micrographs from the Al matrix of the composites with various volume percentages of ND, which clearly indicates that the structure becomes finer as the percentage of ND particles increases. The Al average grain size in different composites was measured using Image-J software, and the results are presented in Table 1. By adding 10 vol% ND, the average grain size of the Al matrix decreased from 143 to 76 μm. The high thermal conductivity of diamond increases the sample's thermal conductivity during solidification, which, in turn, enhances its cooling rate [28]. The increased cooling rate leads to a finer microstructure.

Table 1. Average grain sizes of the Al matrix of the fabricated composites.

ND (vol%)	Average grain size (μm)
0	143
1	118
3	98
10	76

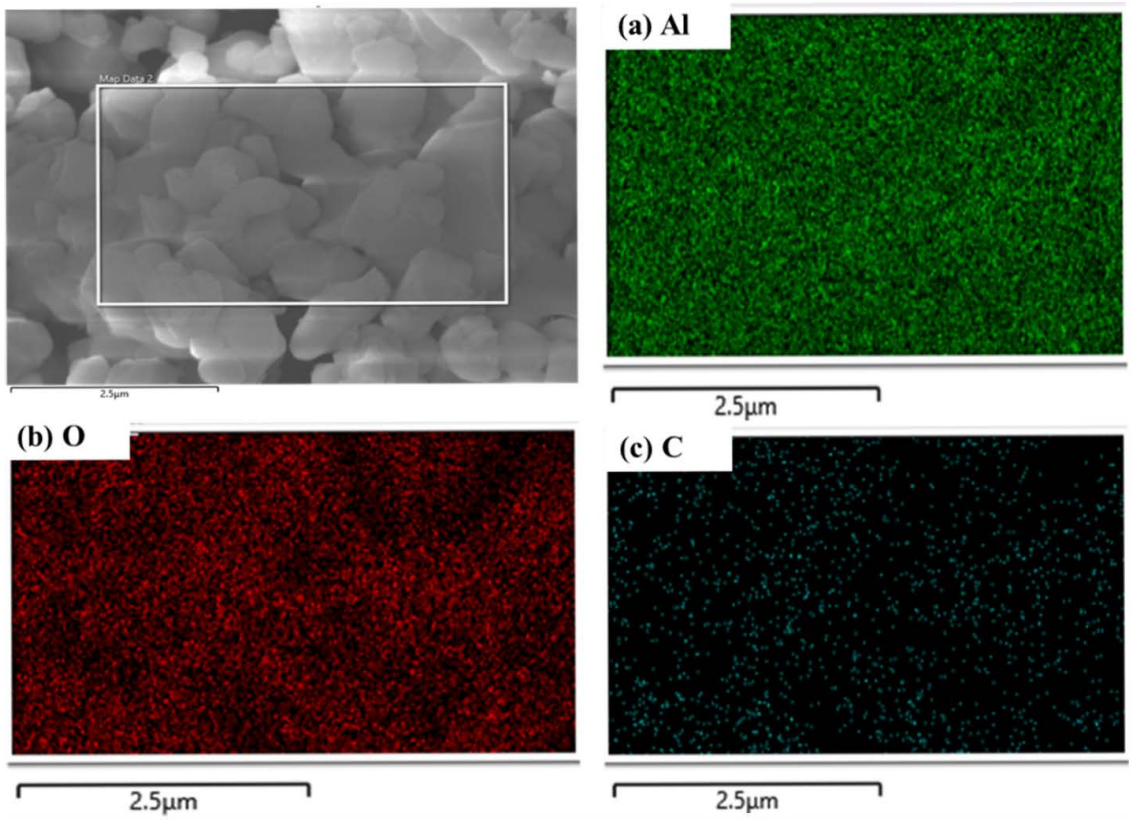

Fig. 4. An elemental distribution map from the ceramic preform containing 10 vol% ND.

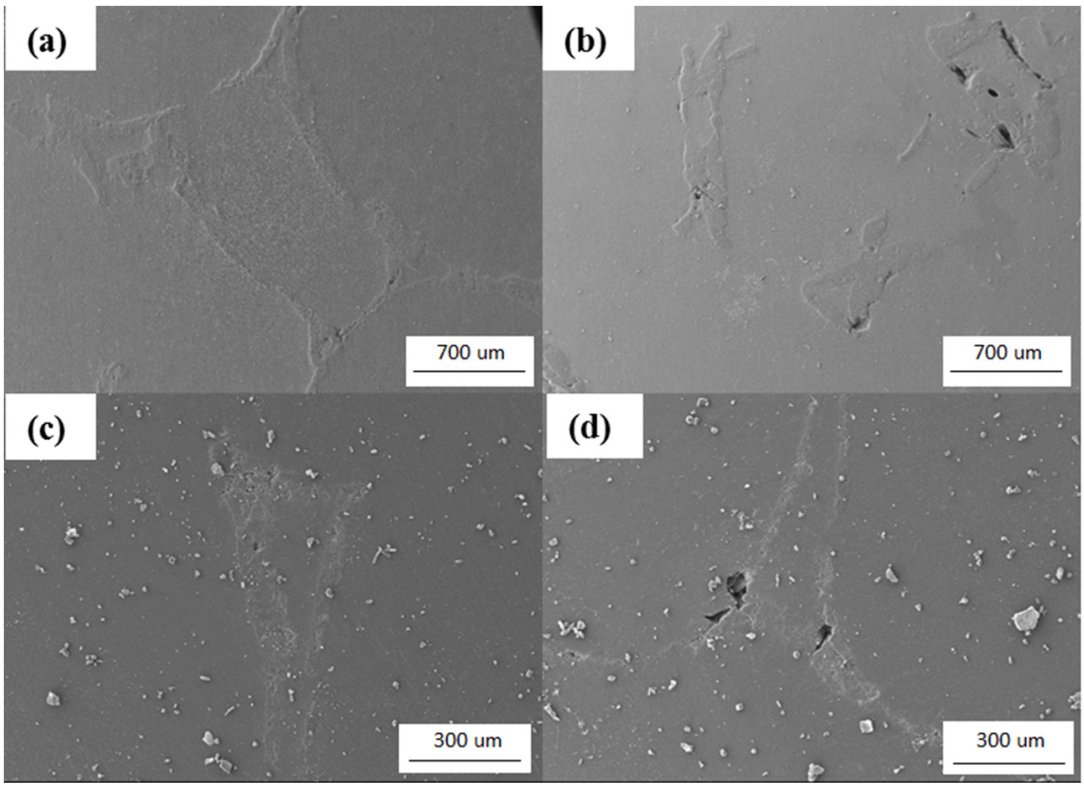

Fig. 5. Low-magnification FE-SEM micrographs from the interpenetrating phases hybrid Al/Al_2O_3-ND composites fabricated with various volume percentages of ND particles, (a) 0, (b) 1, (c) 3, and (d) 10 vol% NDs.

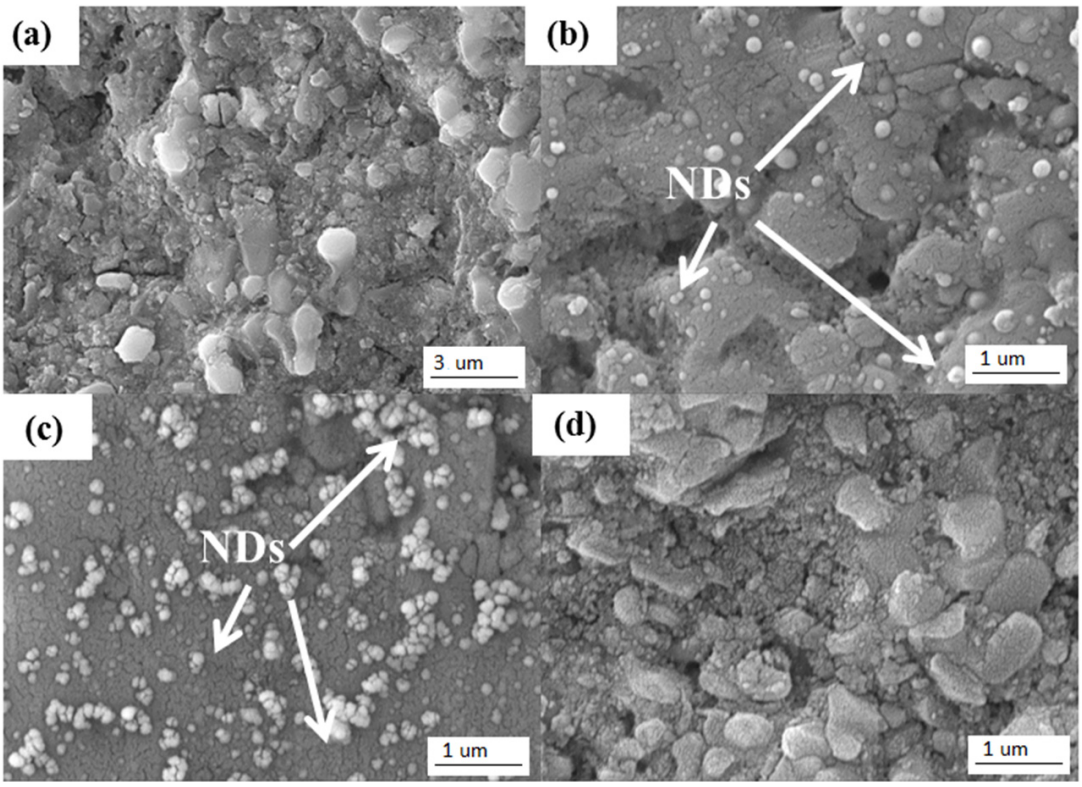

Fig. 6. High-magnification FESEM micrographs from the interpenetrating phases hybrid Al/Al_2O_3-ND composites fabricated with various volume percentages of ND particles, (a) 0, (b) 1, (c) 3, and (d) 10 vol% NDs.

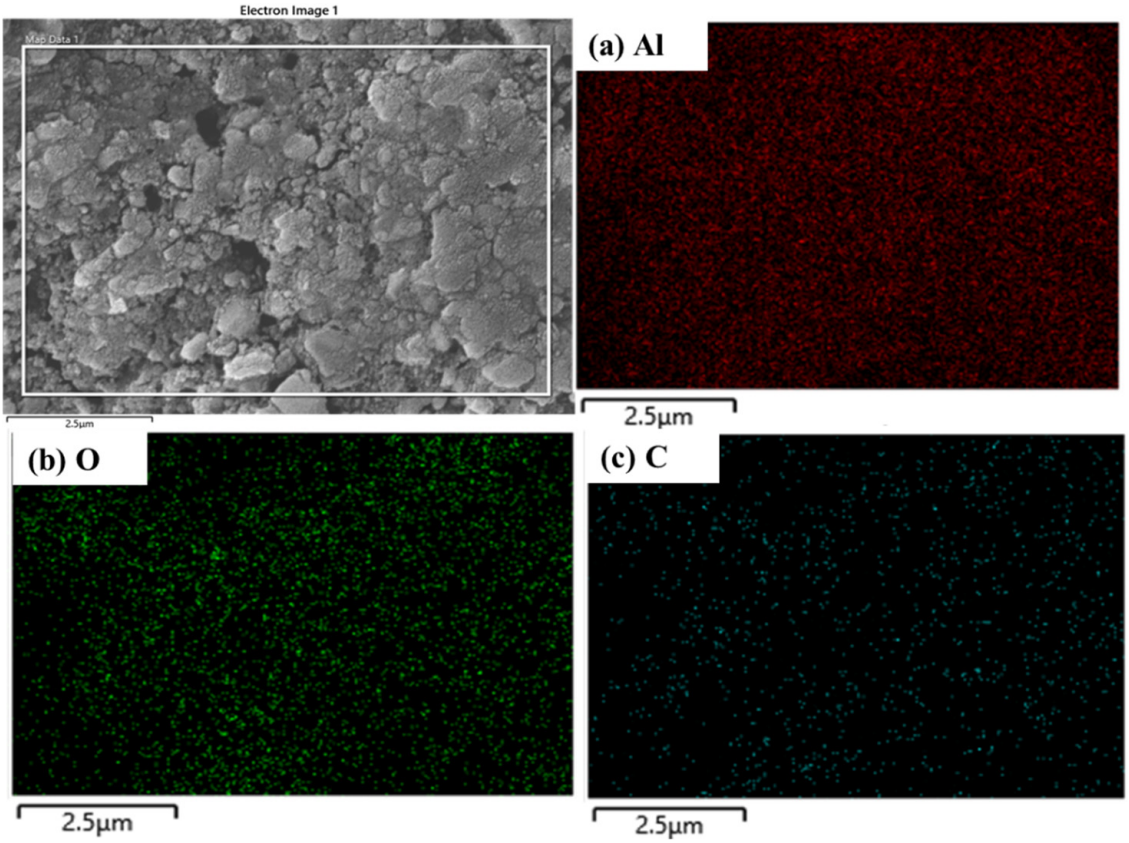

Fig. 7. An elemental distribution map from the interpenetrating phases hybrid Al/Al_2O_3-ND composite containing 10 vol% ND.

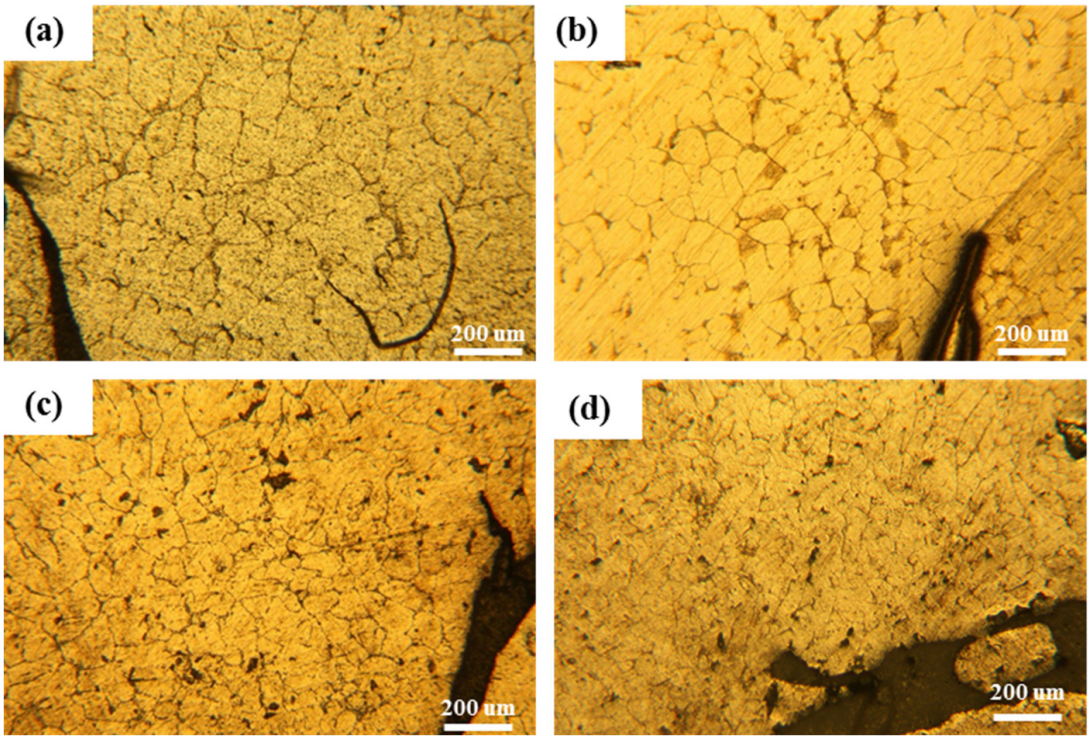

Fig. 8. Optical micrographs from the Al matrix of the composites containing (a) 0, (b) 1, (c) 3, and (d) 10 vol% NDs.

3.3. Hardness behavior

The micro-hardness of the samples was determined using an INNOVA TEST Universal micro-hardness tester. To obtain accurate results, 10 points along the diameter were tested from each sample. Also, an applied load of 500 g was chosen for the indenter of the hardness device. The averaged hardness values are presented in Fig. 9.

The results demonstrate that the hardness of the samples increased with an increase in the volume percentage of ND particles. Incorporating Al_2O_3 into an Al matrix resulted in a significant increase in the composite's hardness, from around 32 to 78 Vickers. The addition of ND further increased the hardness of fabricated composites. As the volume percentage of the ND increased, the hardness of the composite also increased. At 10 vol% of ND, the hardness of the composite increased by 2.3 times compared to the composite without ND. This increase in hardness can be attributed to the distribution of the ND in the reinforcing phase and its hardness.

Fig. 10 illustrates the averaged hardness values of the Al matrix in various fabricated composites. As depicted, the matrix hardness increased as the volume percentage of the ND particles increased. According to the average grain sizes given in Table 1, the finer grain of the Al matrix is likely the main reason for the hardness increase. This can be attributed to the enhanced thermal conductivity resulting from the increased volume percentage of ND. The hardness of the composites increases through the two main strengthening mechanisms. Hence, the hardness of these composites can be explained by the Orowwn mechanism (volume fraction of ND particles) and the Hal-Petch mechanism (grain size) [29].

4. Conclusion

The effect of nanodiamond (ND) particles on the microstructural characteristics and hardness behavior of an interpenetrating phases hybrid aluminum/alumina-nanodiamond metal matrix composite was studied. The following findings were obtained in this work:

1. The hybrid (Al_2O_3 and ND) preforms were successfully sintered in an argon gas atmosphere to avoid ND oxidation.
2. Depending on the ND content in the preforms, the microstructural results showed various ND distributions.
3. The grain size of the Al matrix decreased as the ND volume percentage increased. By adding 10 vol% ND, the average grain size of the Al matrix has decreased from 143 to 76 μm.
4. The ND addition enhanced the hardness of the interpenetrating phases hybrid Al/Al_2O_3 metal matrix composite. For 10 vol% ND addition, the hardness of the composite increased by 2.3 times compared to the composite without ND.

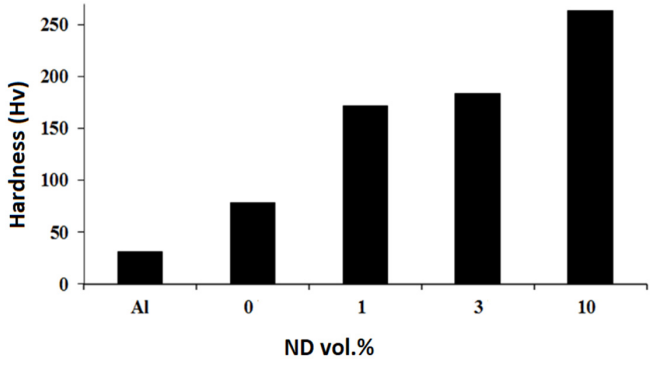

Fig. 9. The averaged hardness values of the fabricated composites based on the volume percentage of ND particles.

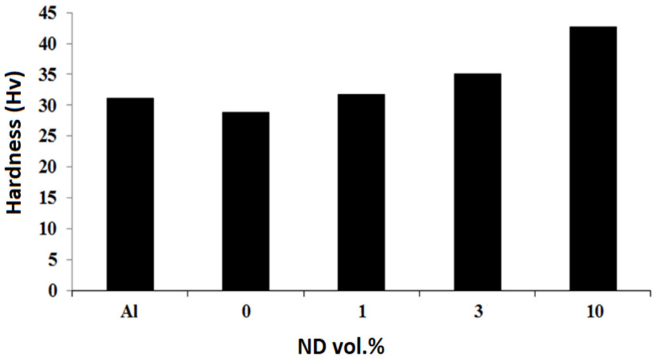

Fig. 10. The averaged hardness values of the Al matrix of the fabricated composites based on the volume percentage of ND particles.

Acknowledgment

The authors wish to acknowledge the Office of Research at the University of Sistan and Baluchestan and the Iran National Science Foundation for the financial support of this work.

Disclosure statement

No potential conflict of interest was reported by the authors.

References

[1] Alipour, M. & Eslami-Farsani, R., (2017). Synthesis and Characterization of Graphene Nanoplatelets Reinforced AA7068 Matrix Nanocomposites Produced by Liquid Metallurgy Route. *Materials Science and Engineering: A, 706*, 71-82. https://doi.org/10.1016/j.msea.2017.08.092

[2] Clarke, D. R. (1992). Interpenetrating Phase Composites. *Journal of the American Ceramic Society, 75*(4), 739-758. https://doi.org/10.1111/j.1151-2916.1992.tb04138.x

[3] Zhou, W., Hu, W., & Zhang, D. (1998). Study on the Making of Metal-Matrix Interpenetrating Phase Composites. *Scripta Materialia, 39*(12), 1743-1748.

https://doi.org/10.1016/S1359-6462(98)00367-4

[4] Daehn, G. S., Starck, B., Xu, L., Elfishawy, K. F., Ringnalda, J., & Fraser, H. L. (1996). Elastic and Plastic Behavior of A Co-Continuous Alumina/Aluminum Composite. *Acta Materialia, 44*(1), 249-261. https://doi.org/10.1016/1359-6454(95)00138-8

[5] Chen, Y., & Chung, D. D. L. (1994). Silicon-Aluminium Network Composites Fabricated by Liquid Metal Infiltration. *Journal of Materials Science, 29*, 6069-6075. https://doi.org/10.1007/BF00354543

[6] Klassen, T., Günther, R., Dickau, B., Gärtner, F., Bartels, A., Bormann, R., & Mecking, H. (1998). Processing and Properties of Intermetallic/Ceramic Composites with Interpenetrating Microstructure. *Journal of the American Ceramic Society, 81*(9), 2504-2506. https://doi.org/10.1111/j.1151-2916.1998.tb02654.x

[7] Mattern, A., Huchler, B., Staudenecker, D., Oberacker, R., Nagel, A., & Hoffmann, M. J. (2004). Preparation of Interpenetrating Ceramic–Metal Composites. J*ournal of the European ceramic society, 24*(12), 3399-3408. https://doi.org/10.1016/j.jeurceramsoc.2003.10.030

[8] Hammel, E. C., Ighodaro, O. R., & Okoli, O. I. (2014). Processing and Properties of Advanced Porous Ceramics: An Application Based Review. *Ceramics International, 40*(10), 15351-15370. https://doi.org/10.1016/j.ceramint.2014.06.095

[9] Horny, D., Schukraft, J., Weidenmann, K. A., & Schulz, K. (2020). Numerical and Experimental Characterization of Elastic Properties of A Novel, Highly Homogeneous Interpenetrating Metal Ceramic Composite. *Advanced Engineering Materials, 22*(7), 1901556. https://doi.org/10.1002/adem.201901556

[10] Konopka, K., & Szafran, M. (2006). Fabrication of Al_2O_3–Al Composites by Infiltration Method and Their Characteristic. *Journal of Materials Processing Technology, 175*(1-3), 266-270. https://doi.org/10.1016/j.jmatprotec.2005.04.046

[11] Scherm, F., Völkl, R., Neubrand, A., Bosbach, F., & Glatzel, U. (2010). Mechanical Characterisation of Interpenetrating Network Metal–Ceramic Composites. *Materials Science and Engineering: A, 527*(4-5), 1260-1265. https://doi.org/10.1016/j.msea.2009.09.063

[12] Dolata, A. J. (2016). Fabrication and Structure Characterization of Alumina-Aluminum Interpenetrating Phase Composites. *Journal of Materials Engineering and Performance, 25*, 3098-3106. https://doi.org/10.1007/s11665-016-1901-2

[13] Binner, J., Chang, H., & Higginson, R. (2009). Processing of Ceramic-Metal Interpenetrating Composites. *Journal of the European Ceramic Society, 29*(5), 837-842. https://doi.org/10.1016/j.jeurceramsoc.2008.07.034

[14] San Marchi, C., Kouzeli, M., Rao, R., Lewis, J. A., & Dunand, D. C. (2003). Alumina–Aluminum Interpenetrating Phase Composites with Three-Dimensional Periodic Architecture. *Scripta Materialia, 49*(9), 861-866. https://doi.org/10.1016/S1359-6462(03)00441-X

[15] Oliveira, F. C., Dias, S., Vaz, M. F., & Fernandes, J. C. (2006). Behaviour of Open-Cell Cordierite Foams Under Compression. *Journal of the European Ceramic Society, 26*(1-2), 179-186. https://doi.org/10.1016/j.jeurceramsoc.2004.10.008

[16] Roy, S., Schell, K. G., Bucharsky, E. C., Weidenmann, K. A., Wanner, A., & Hoffmann, M. J. (2019). Processing and Characterization of Elastic and Thermal Expansion Behavior of Interpenetrating Al12Si/Alumina Composites. Materials Science and Engineering: A, 743, 339-348. https://doi.org/10.1016/j.msea.2018.11.100

[17] Kota, N., Sai Charan, M., Laha, T., Roy, S. (2022). Review on Development of Metal/Ceramic Interpenetrating Phase Composites and Critical Analysis of Their Properties. *Ceramics International, 48*(2), 1451-1483. https://doi.org/10.1016/j.ceramint.2021.09.232

[18] Roudini, G., Tavangar, R., Weber, L., & Mortensen, A. (2010). Influence of Reinforcement Contiguity on the Thermal Expansion of Alumina Particle Reinforced Aluminum Composites. *International Journal of Materials Research, 101*(9), 1113-1120. https://doi.org/10.3139/146.110388

[19] Kouzeli, M. & Dunand, D. C. (2003). Effect of Reinforcement Connectivity on the Elasto-Plastic Behavior of Aluminum Composites Containing Sub-Micron Alumina Particles. *Acta Materialia, 51*, 6105-6121. https://doi.org/10.1016/S1359-6454(03)00431-2

[20] Parr, M. D., & Reinhard, D. K. (2006). Electrical Properties of Thin Nanocrystalline Diamond Based Structures. *Diamond and Related Materials, 15*(2-3), 207-211. https://doi.org/10.1016/j.diamond.2005.10.019

[21] Das, P., Paul, S., & Bandyopadhyay, P. P. (2018). HVOF Sprayed Diamond Reinforced Nano-Structured Bronze Coatings. *Journal of Alloys and Compounds, 746*, 361-369. https://doi.org/10.1016/j.jallcom.2018.02.307

[22] Che, Z., Li, J., Wang, Q., Wang, L., Zhang, H., Zhang, Y., & Kim, M. J. (2018). The Formation of Atomic-Level Interfacial Layer and Its Effect on Thermal Conductivity of W-Coated Diamond Particles Reinforced Al Matrix Composites. *Composites Part A: Applied Science and Manufacturing, 107*, 164-170. https://doi.org/10.1016/j.compositesa.2018.01.002

[23] Abyzov, A. M., Shakhov, F. M., Averkin, A. I., & Nikolaev, V. I. (2015). Mechanical Properties of

Conductivity. *Materials & Design, 87*, 527-539. https://doi.org/10.1016/j.matdes.2015.08.048

[24] Chen, C., Xie, Y., Yan, X., Ahmed, M., Lupoi, R., Wang, J., & Yin, S. (2020). Tribological Properties of Al/Diamond Composites Produced by Cold Spray Additive Manufacturing. *Additive Manufacturing, 36*, 101434. https://doi.org/10.1016/j.addma.2020.101434

[25] Jiao, Z., Kang, H., Zhou, B., Kang, A., Wang, X., Li, H., & Wei, Q. (2022). Research Progress of Diamond/Aluminum Composite Interface Design. *Functional Diamond, 2*(1), 25-39. https://doi.org/10.1080/26941112.2022.2050953

[26] Xie, H., Chen, Y., Zhang, T., Zhao, N., Shi, C., He, C., & Liu, E. (2020). Adhesion, Bonding and Mechanical Properties of Mo Doped Diamond/Al (Cu) Interfaces: A First Principles Study. *Applied Surface Science, 527*, 146817. https://doi.org/10.1016/j.apsusc.2020.146817

[27] Khosravi, H., Eslami-Farsani, R., & Askari-Paykani, M. (2014). Modeling and Optimization of Cooling Slope Process Parameters for Semi-Solid Casting of A356 Al Alloy. *Transactions of Nonferrous Metals Society of China, 24*(4), 961-968. https://doi.org/10.1016/S1003-6326(14)63149-6

[28] Zhang, Y., Rhee, K. Y., Hui, D., & Park, S. (2018). A Critical Review of Nanodiamond Based Nanocomposites: Synthesis, Properties and Applications. *Composites Part B: Engineering, 143*, 19-27. https://doi.org/10.1016/j.compositesb.2018.01.028

[29] Miller, W. S., & Humphreys, F. J., (1991). Strengthening Mechanisms in Particulate Metal Matrix Composites. *Scripta Metallurgica et Materialia, 25*(1), 33-38. https://doi.org/10.1016/0956-716X(91)90349-6

Additional information

Correspondence and requests for materials should be addressed to G. Roudini.

HOW TO CITE THIS ARTICLE

Zeinali Moghaddam, H.; Roudini, G.; Khosravi, H. (2023). Fabrication Method, Microstructural Characteristics, and Hardness Behavior of An Interpenetrating Phases Hybrid Aluminum/Alumina-Nanodiamond Composite. *J. Part. Sci. Technol. 9(2) 63-71.*

DOI: 10.22104/JPST.2023.6538.1244
URL: https://jpst.irost.ir/article_1338.html